Dynamics of intraoceanic subduction initiation: 2. Suprasubduction zone ophiolite formation and metamorphic sole exhumation in context of absolute plate motions

Douwe J. J. van Hinsbergen[1], Kalijn Peters[1], Marco Maffione[1], Wim Spakman[1,2], Carl Guilmette[3], Cedric Thieulot[1,2], Oliver Plümper[1], Derya Gürer[1], Fraukje M. Brouwer[4], Ercan Aldanmaz[5], and Nuretdin Kaymakcı[6]

[1]Department of Earth Sciences, University of Utrecht, Utrecht, Netherlands, [2]Centre for Earth Evolution and Dynamics, Oslo, Norway, [3]Department of Geology and Geological Engineering, Laval University, Quebec City, Québec, Canada, [4]Faculty of Earth and Life Sciences, VU University, Amsterdam, Netherlands, [5]Department of Geology, University of Kocaeli, Izmit, Turkey, [6]Department of Geological Engineering, Middle East Technical University, Ankara, Turkey

Abstract Analyzing subduction initiation is key for understanding the coupling between plate tectonics and the underlying mantle. Here we focus on suprasubduction zone (SSZ) ophiolites and how their formation links to intraoceanic subduction initiation in an absolute plate motion frame. SSZ ophiolites form the majority of exposed oceanic lithosphere fragments and are widely recognized to have formed during intraoceanic subduction initiation. Structural, petrological, geochemical, and plate kinematic constraints on their kinematic evolution show that SSZ crust forms at fore-arc spreading centers at the expense of a mantle wedge, thereby flattening the nascent slab. This leads to the typical inverted pressure gradients found in metamorphic soles that form at the subduction plate contact below and during SSZ crust crystallization. Former spreading centers are preserved in forearcs when subduction initiates along transform faults or off-ridge oceanic detachments. We show how these are reactivated when subduction initiates in the absolute plate motion direction of the inverting weakness zone. Upon inception of slab pull due to, e.g., eclogitization, the sole is separated from the slab, remains welded to the thinned overriding plate lithosphere, and can become intruded by mafic dikes upon asthenospheric influx into the mantle wedge. We propound that most ophiolites thus formed under special geodynamic circumstances and may not be representative of normal oceanic crust. Our study highlights how far-field geodynamic processes and absolute plate motions may force intraoceanic subduction initiation as key toward advancing our understanding of the entire plate tectonic cycle.

1. Introduction

Plate tectonic theory describes the Earth's lithosphere as a mosaic of rigid plates moving along discrete plate boundaries: subduction zones, mid-oceanic ridges, and transform faults [*McKenzie and Parker*, 1967]. Plates and plate boundaries are transient features. For instance, nearly half of today's subduction zones formed in the last 65 Myr [*Gurnis et al.*, 2004]. Initiation of new subduction zones must therefore be a common and episodically recurring process that is fundamental to the plate tectonic cycle of creation and destruction of oceanic plates. The causes and mechanisms of subduction initiation, however, are particularly difficult to unravel from the geological record given the plate-destructive nature of subduction zones.

Ophiolites are oceanic lithosphere fragments that are exposed above sea level, normally because they became uplifted in the hanging wall of a cross-lithospheric thrust that is typically inferred to be a subduction zone [*Dewey*, 1976], although other typical features of subduction zones, such as volcanic arcs or exhumed high-pressure, low-temperature metamorphic rocks, are not always present. Ophiolites are thought to constitute the best geological archives of the subduction initiation process. Ophiolite belts occur in many mountain ranges and result from underthrusting of a passive continental margin or an accretionary prism below oceanic lithosphere following intraoceanic subduction, a process widely referred to as "ophiolite obduction" [*Coleman*, 1971; *Dewey and Bird*, 1971; *Stoneley*, 1975; *Dewey*, 1976; *Atkinson*, 1976]. The across-strike width of a preserved ophiolite belt normally corresponds to the distance over which the

overriding oceanic plate was underthrust by a buoyant continental margin, arc, or accretionary wedge, which is typically less than ∼200 km [*McQuarrie and van Hinsbergen*, 2013]. After the formation of the cross-lithospheric thrust fault/subduction zone that led to their uplift above sea level, ophiolite belts thus represent the leading edge of a (former) overriding plate with oceanic lithosphere (Figure 1) [*Dewey*, 1976; *Moores*, 1982; *Wakabayashi and Dilek*, 2000].

The oceanic crust of ophiolites once formed at a spreading center and may preserve fossil transform faults (i.e., fracture zones) and spreading axes [e.g., *Simonian and Gass*, 1978; *MacLeod et al.*, 1990], offering unique opportunity to study seafloor spreading dynamics [*Hess*, 1965; *Dewey et al.*, 1973; *Moores*, 1982; *Nicolas*, 1989; *Nicolas et al.*, 2000]. With the advent of geochemistry, possibilities arose to compare the geochemical composition of ophiolites with modern-day oceanic basins in different tectonic settings, e.g., mid-ocean ridges, back-arc basins, or volcanic arcs, and to develop geochemical proxies for tectonic environments of ophiolite formation. Aside ophiolites with geochemical signatures similar to Mid-Ocean Ridge Basalts (MORB), or Back-Arc Basin Basalts (BABB), a third, abundant class of ophiolites was recognized that has a volcanic arc signature [*Miyashiro*, 1973]. Such a signature would suggest that those ophiolites formed in the narrow, few hundred kilometer wide zone close to a trench where the mantle is enriched by subduction-related fluids. This class of ophiolites became known as "suprasubduction zone" (SSZ) ophiolites [*Casey and Dewey*, 1984; *Pearce et al.*, 1984; *Shervais*, 2001; *Stern*, 2004] and has been widely studied because their specific tectonic setting is difficult to explain. Where MOR or BAB-derived ophiolites merely require the formation of a cross-lithospheric thrust/subduction zone within an ocean or back arc, SSZ ophiolites require the formation of a spreading center immediately adjacent to a subduction zone, i.e., in a highly convergent setting.

Approximately a decade after SSZ ophiolites were formally defined, *Stern and Bloomer* [1992] pointed out, on the basis of geochemical and thermodynamic arguments, that the process of SSZ ophiolitic crust production appears to be restricted to the first ∼10 Myr of a subduction zone's lifetime, and these authors therefore linked the formation of SSZ ophiolites to the subduction initiation process. This notion was consistent with conclusions drawn from an additional puzzling feature of many ophiolites, frequently with a SSZ-type geochemistry: metamorphic soles. Metamorphic soles form intensely foliated and sheared, up to a few hundred meter thick sequences of metamorphosed basalts and pelagic sediments welded to the base of many SSZ ophiolites. Soles are interpreted to derive from sediments from the top of a nascent oceanic slab that accreted to the base of the still hot overriding plate in the early stages of intraoceanic thrusting [*Casey and Dewey*, 1984; *Hacker*, 1990; *Wakabayashi and Dilek*, 2000; *Dewey and Casey*, 2011].

If SSZ ophiolites and their soles are indeed closely related to the subduction initiation process, they may hold the key toward understanding how subduction zones form [*Wakabayashi et al.*, 2010; *Dewey and Casey*, 2011, 2013; *Dilek and Furnes*, 2011; *Stern et al.*, 2012; *MacLeod et al.*, 2013]. Many outstanding problems remain, however: How can intraoceanic subduction initiation be associated with formation of fore-arc spreading centers? Can metamorphic sole formation and SSZ crust formation in the overriding plate be synchronous processes related to subduction initiation? How were the high-grade metamorphic rocks of these soles exhumed back to the surface?

Here we review the key characteristics of SSZ-type ophiolites and metamorphic soles that provide quantitative boundary conditions for the geodynamic setting in which they formed. Because most outstanding questions focus on relative motions between elements of the ophiolite sequence, we consider the subduction initiation, SSZ ophiolite formation, and metamorphic sole exhumation processes in an absolute plate kinematic context. We then evaluate geodynamic models of subduction initiation and formation of fore-arc spreading centers and propose a scenario that unifies the tectonic, metamorphic, and magmatic evolution of the early stages of intraoceanic subduction. With this, we identify key targets to further the fundamental understanding of plate tectonics and the lessons contained in ophiolite geology and geochemistry.

2. Suprasubduction Zone Ophiolites

The most complete ophiolites contain a so-called "Penrose" sequence [*Geotimes*, 1972], comprising upper mantle harzburgitic peridotite, lower crust layered gabbro, and upper crust sheeted dykes, pillow lavas and deep-marine cover sediments. Only ∼10% of ophiolites show this entire sequence and especially the crustal
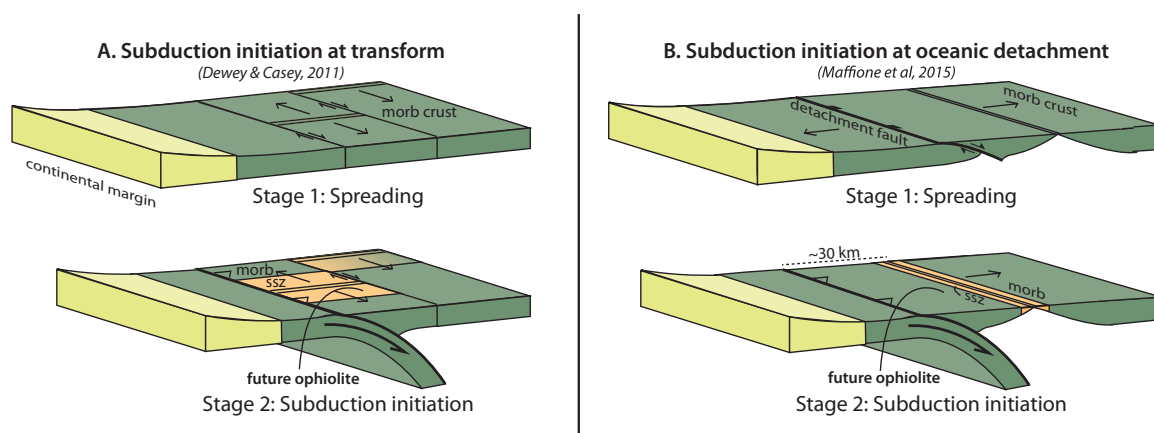
Figure 1. Two proposed modes of subduction initiation, along (a) a transform-fracture zone [*Dewey and Casey*, 2011] or (b) an oceanic detachment fault [*Maffione et al.*, 2015a] in which a former mid-oceanic ridge is preserved in the fore arc of a newly formed subduction zone. Continued spreading or reactivation of this ridge during the subduction initiation process generates SSZ oceanic crust.

components are frequently thin or missing, e.g., depending on the efficiency of melt extraction from the mantle below the ridge [*Shervais*, 2001; *Dilek and Furnes*, 2011]. In particular, while the "Penrose" sequence schematically suggested that the oceanic crust is 6–8 km thick, as inferred from seismic observations of the modern ocean floor [e.g., *Moores*, 1982], the thickest magmatic crust found in ophiolites is ∼3 km [*Nicolas et al.*, 2000]. Since the plate tectonic revolution, ophiolites have been recognized as on-land analogues of the oceanic lithosphere formed at mid-ocean ridges, until geochemical studies amassed enough evidence to assert that many ophiolites must have formed above subduction zones (for a comprehensive review, see *Pearce* [2003]).

Evidence for the SSZ nature of ophiolites comes from geochemical fingerprinting techniques: as a consequence of slab-derived fluids, the lithospheric mantle of SSZ ophiolites has experienced a higher degree of depletion due to melt extraction than mantle below normal mid-ocean ridges [e.g., *Hirose and Kawamoto*, 1995]. Immobile element fingerprinting of lavas, where incompatible (Ti, Zr, and Y) and compatible elements (Cr, Ni, and Mg) are compared, reliably identifies enhanced mantle melting due to subduction zone fluid input [*Shervais*, 1982; *Pearce et al.*, 1984]. The element Th is key, being enriched in arc lavas and mobilized in subduction zones, but remaining immobile until temperatures close to melting temperatures of the source sediments are reached [*Johnson and Plank*, 1999]. Additionally, melting preferentially extracts Al from chrome spinel, a common upper mantle mineral, increasing the Cr-number as melting progresses. SSZ ophiolites typically show very high Cr-numbers [*Dick and Bullen*, 1984].

At normal mid-ocean ridges, the upper mantle is generally depleted by ∼10–15% partial melting and the extracted melt has a "Mid-Ocean Ridge Basalt" (MORB) composition [*Pagé et al.*, 2009]. Subsequent fluid-assisted melting may deplete mantle wedge peridotite by an additional 15–20% partial melting ("ultradepletion") which extracts melt with a SSZ crustal composition [*Pagé et al.*, 2009], so-called boninites. Boninites result from mantle melting at low pressures (3–7 kbar, i.e., ∼10–20 km depth) [*Kostopoulos and Murton*, 1992], due to unusually hot conditions within the mantle wedge during the first 5–10 Myr after subduction initiation [*Stern et al.*, 2012]. Boninites may therefore relate to subduction initiation close to a mid-oceanic ridge [e.g., *Hickey and Frey*, 1982; *Pearce et al.*, 1992; *Stern and Bloomer*, 1992; *Ishikawa et al.*, 2002; *Stern et al.*, 2012]. After 5–10 Myr, the mantle wedge cools, is serpentinized, boninite formation stops, and a stable volcanic arc forms at a larger distance from the trench placing the SSZ crust in a forearc position [e.g., *Stern and Bloomer*, 1992; *Rioux et al.*, 2007; *Stern et al.*, 2012].

It would be logical to infer that the melts that produced the SSZ oceanic crust found in ophiolites have been derived from their underlying, ultradepleted mantle. The thickest ophiolites, however, are only 10–12 km thick, i.e., shallower than the depths at which boninites were extracted from the mantle wedge [e.g., *Pagé et al.*, 2009]. The modern ultradepleted mantle sections can thus only be the source of the ophiolite's crust if the ophiolite sequence was significantly thinned and attenuated after boninite generation and

before obduction [*Casey and Dewey*, 1984; *Hacker and Gnos*, 1997; *Dewey and Casey*, 2013]. We will address this later in the paper, but for now we note that (i) to form SSZ oceanic crust, a spreading center must form, continue, or resume activity in the early stages of subduction above the nascent slab and (ii) if ultradepletion after subduction initiation exceeds potential refertilization, the ophiolite's mantle reservoir empties faster than it is replenished: the volume of the mantle reservoir above the nascent slab (i.e., the mantle wedge) then decreases during SSZ spreading to form SSZ oceanic crust.

3. Metamorphic Soles

Metamorphic soles are up to 500 m thick, intensely sheared mafic magmatic and sedimentary rock sequences found at the base of ophiolitic mantle sections [*Malpas*, 1979; *Searle and Malpas*, 1980; *Boudier and Coleman*, 1981; *Boudier et al.*, 1988; *Nicolas et al.*, 2000; *Çelik et al.*, 2006; *Dewey and Casey*, 2011, 2013], extending tens to more than a hundred kilometers away from the obduction front. The most complete soles consist from the top down of garnet-amphibolites or -granulites, amphibolites, greenschists, and anchimetamorphic pillow basalts and radiolarites.

Climax metamorphic conditions of the garnet-amphibolites or -granulites from the top of soles are up to ~850–900°C and 10–15 kbar, equivalent to ~30–45 km depth [*Dilek and Whitney*, 1997; *Hacker and Gnos*, 1997; *Wakabayashi and Dilek*, 2000; *Elitok and Drüppel*, 2008; *Guilmette et al.*, 2008; *Myhill*, 2011]. In a mature subduction zone, temperatures of 850–900°C are much higher than expected at pressures of 10–15 kbar; such high temperatures require that the mantle section of the ophiolite was hot when sole formation started. Soles are consequently thought to form in the first few Myr of subduction starting close to, or at a mid-oceanic ridge [*Hacker*, 1990] (Figure 1). Mantle sections of many ophiolites, away from the sole, preserve fabrics suggesting deformation at temperatures well over 1000°C [*Nicolas et al.*, 2000], although it is frequently difficult to determine whether this deformation pre or postdated subduction initiation. However, in the Vourinos ophiolite of Greece these high-temperature fabrics formed in an ultradepleted mantle section [*Rassios and Moores*, 2006; *Kapsiotis*, 2014], and since ultradepletion occurs in a mantle wedge as a result of subduction-related fluid addition, these temperatures must have existed after subduction initiation, above the slab, and above the metamorphic sole, as is also required to partially melt that mantle so as to ultradeplete it.

Where constrained, and considering large uncertainties, pressures of recrystallization of the peridotites above the sole are similar to the 10–15 kbar estimated from the top of the sole [*Spray et al.*, 1984; *Jamieson*, 1986]. In addition, aluminum and manganese-rich, granulite-facies metasedimentary and metabasic rocks are found enclosed within the mantle section of the Semail ophiolite in the United Arab Emirates (UAE) section, where they formed at 800–850°C and 6.5–9 kbar [*Gnos and Kurz*, 1994; *Gnos and Peters*, 1995]. These constraints suggest that in the early stages of sole formation, a ~30–45 km thick mantle section with very high temperatures must have existed to which rocks from the top of an incipient slab were welded forming the upper levels of the metamorphic sole, or within which they were injected, in the UAE case. Paradoxically, no ophiolite is presently thicker than ~10–12 km, and most are much thinner [*Hacker and Gnos*, 1997; *Dilek and Furnes*, 2011; *Dewey and Casey*, 2013].

The basal section of a metamorphic sole, however, exposes rocks with lower peak pressure and temperature conditions than those found in the uppermost (amphibolitic) intervals. Typical PT evolutions for different levels in a sole's tectonostratigraphy, based on well-studied examples of, e.g., the Bay of Islands ophiolite of eastern Canada [*Jamieson*, 1980; *Dewey and Casey*, 2013], the Semail ophiolite of Oman [*Hacker and Gnos*, 1997], the Muslim Bagh ophiolite of Pakistan [*Mahmood et al.*, 1995; *Kakar et al.*, 2014], several Neotethyan ophiolites in Turkey [*Dilek and Whitney*, 1997; *Plunder et al.*, 2013], and the Balkan-Hellenic ophiolites [*Dimo-Lahitte et al.*, 2001; *Myhill*, 2011] are shown in Figure 2. Since normally no pseudomorphs after higher-grade minerals are found in lower-grade levels, and lower-grade shear zones do not anastomose around higher-grade relics, deeper levels likely represent allochtonous rocks that were accreted to the base of the sole at lower peak metamorphic conditions that fall on the structurally higher level's retrograde paths [*Hacker and Gnos*, 1997; *Dewey and Casey*, 2013]. In several Anatolian metamorphic soles, static glaucophane overgrowths over amphibolite-facies sole rocks [*Dilek and Whitney*, 1997; *Plunder et al.*, 2013] indicate that retrograde paths can pass through the blueschist field (Figure 2). Although thus far unconstrained, the age of climax metamorphism of different levels of a single sole likely decreases downward.
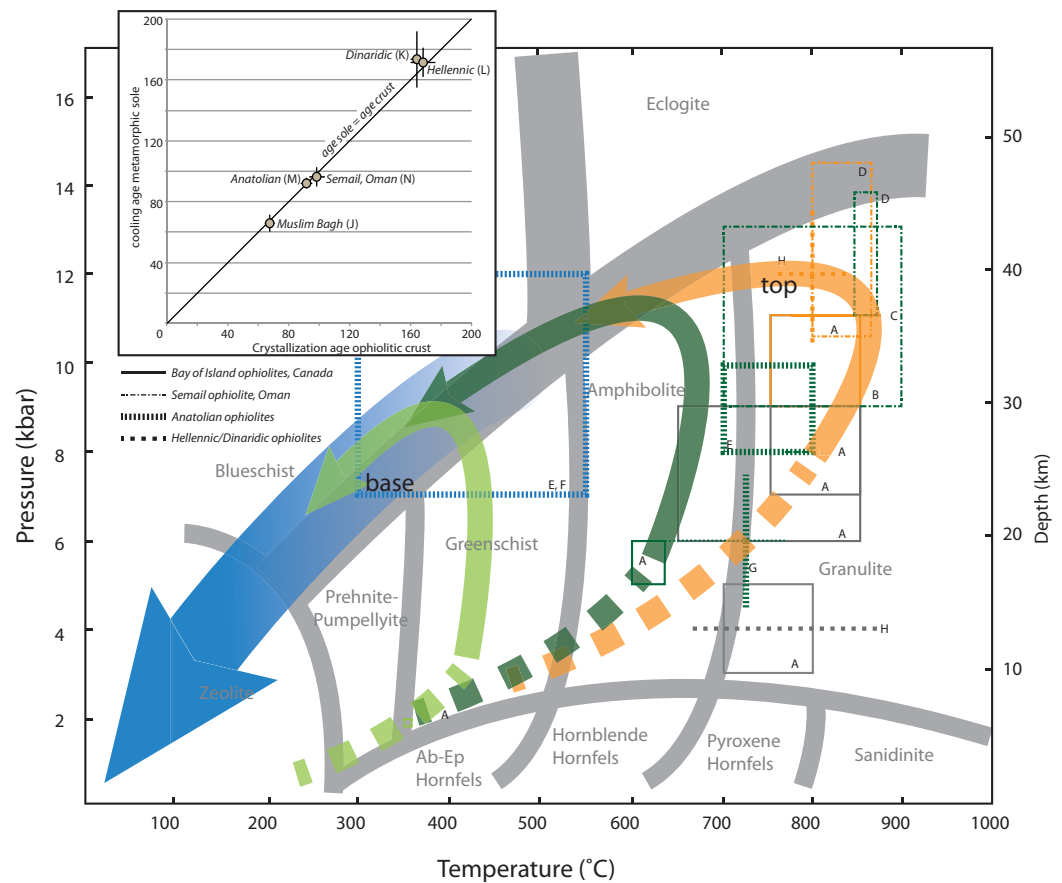
Figure 2. Conceptual pressure-temperature paths of different levels of metamorphic soles based on four well-studied sole systems. The structurally higher part of the sole underwent a longer, deeper, and hotter evolution than the structurally lower part, which was welded to the sole during decompression and cooling of the upper part. Key to references: A = *Dewey and Casey* [2013, and references therein]; B = *Gnos* [1998]; C = *Hacker and Gnos* [1997]; D = *Searle and Cox* [2002]; E = *Plunder et al.* [2013]; F = *Myhill* [2011]; G = *Dilek and Whitney* [1997]; H = *Elitok and Drüppel* [2008]; J = *Mahmood et al.* [1995]; K = *Dimo-Lahitte et al.* [2001] and *Šoštarić et al.* [2014]; L = *Spray et al.* [1984]; M = *Çelik et al.* [2006] and *Çelik* [2008]; N = *Tilton et al.* [1981], *Hacker* [1994], *Hacker et al.* [1996], *Warren et al.* [2005], and *Rioux et al.* [2012, 2013].

The structurally lowest parts of metamorphic soles in places consist of very low grade to essentially nonmetamorphic radiolarian cherts, pelagic carbonates, and pillow basalts.

Metamorphic soles thus start forming at depths up to ∼45 km below a hot mantle, and subsequently grow by accretion to their base during decompression and cooling to even nonmetamorphic conditions, while maintaining a widespread coverage below the fore arc, up to 100 km or more away from the trench. ^{40}Ar/^{39}Ar amphibole cooling ages for the sole typically overlap with or are a few million years younger than crustal crystallization ages of the overlying SSZ ophiolites [*Hacker*, 1994; *Hacker et al.*, 1996; *Wakabayashi and Dilek*, 2000; *Dimo-Lahitte et al.*, 2001; *Çelik et al.*, 2006; *Guilmette et al.*, 2009, 2012; *Hébert et al.*, 2012; *Rioux et al.* 2012, 2013; *Šoštarić et al.*, 2014]. Exhumation and cooling of metamorphic soles thus likely starts during the spreading that ultradepletes the mantle wedge and produces the ophiolitic SSZ crust above the sole, and continues a few million years beyond the magmatic spreading stage when exhumation and cooling of the sole occurs at temperatures much lower than those that allow mantle melting.

In particular in the Neotethyan ophiolite belt of Oman and Turkey, metamorphic soles and their contact with the mantle section above are in places cut by undeformed mafic dykes with a volcanic arc geochemical signature [*Lytwyn and Casey*, 1995; *Hacker et al.*, 1996; *Hacker and Gnos*, 1997; *Çelik*, 2007]. The ^{40}Ar/^{39}Ar ages of these dykes are 1–20 Myr younger than the cooling ages of the sole they cut [*Lytwyn and Casey*, 1995; *Hacker et al.*, 1996; *Hacker and Gnos*, 1997; *Çelik*, 2008]. This shows that following sole formation and exhumation, mantle material was introduced between the slab and the sole, producing melts for extended time periods.

4. Subduction Initiation and Plate Kinematics

Formation of SSZ ophiolites with boninites is commonly believed to occur at the expense of hot mantle, shortly after intraoceanic subduction initiation [e.g., *Hickey and Frey*, 1982; *Pearce et al.*, 1992; *Kostopoulos and Murton*, 1992; *Ishikawa et al.*, 2002; *Stern et al.*, 2012]. A geodynamic scenario of subduction initiation should therefore explain why a spreading center forms in above the mantle wedge close to the nascent subduction zone [*Pearce*, 2003]. Plate kinematic concepts were put forward to explain how preexisting spreading ridges can be preserved in a fore arc after subduction initiation along (i) a transform fault-fracture zone [*Dewey and Casey*, 2011] and (ii) oceanic detachment faults adjacent to a mid-oceanic ridge [*Maffione et al.*, 2015a] (Figure 1).

Dewey and Casey [2011] showed how subduction initiation along a transform fault-fracture zone preserves a ridge at the leading edge of the overriding plate, perpendicular to the trench (Figure 1). Ongoing spreading at that ridge during subduction initiation would generate SSZ oceanic crust. Ophiolites formed this way should display an along-trench change from MORB/BABB to SSZ crust and back, the transition corresponding to the timing of subduction initiation, alongside a diachronicity in crustal ages along the ophiolite belt. This scenario may apply to the Caledonian ophiolite belt of Newfoundland [*Dewey and Casey*, 2013] and to subduction at the Marianas trench [*Dewey and Casey*, 2011], perhaps together with mantle upwelling along the nascent subduction zone parallel to the former transform [*Stern*, 2004; *Stern et al.*, 2012]. Trench-parallel fore-arc spreading may also result from strain partitioning above oblique subduction zones, leading to SSZ crust generation in pull-apart basins along fore-arc sliver-bounding transform faults. Examples include the Andaman Sea at the India-SE Asia plate boundary [*Moores et al.*, 1984] and the uppermost Cretaceous ophiolites of Pakistan at the India-Arabia plate boundary [*Mahmood et al.*, 1995; *Gnos et al.*, 1997; *Gaina et al.*, 2015. Would subduction initiate spontaneously along transform fault-fracture zones, then subduction-induced extension could be directed orthogonal to the trench, as postulated for the Izu-Bonin fore arc [*Stern*, 2004; *Stern et al.*, 2012]. Since the older lithosphere along the transform (i.e., farthest from the ridge) is the most dense and would hence become the downgoing plate, spontaneous formation of subduction along a transform fault-fracture zone would involve a subduction polarity change at the ridge, where the age relationship of the two sides of a transform-fracture zone flips. No examples of such a flip are known. More importantly, spontaneous collapse models were criticized in numerical modeling studies, since oceanic lithosphere that is old enough to be denser than the mantle has a high resistance against plate bending that would prevent subduction to nucleate spontaneously [*Toth and Gurnis*, 1998; *Hall et al.*, 2003; *Gurnis et al.*, 2004].

Intraoceanic subduction may also start parallel to mid-ocean ridges [*Boudier et al.*, 1988; *Hacker*, 1991, 1994; *Wakabayashi and Dilek*, 2000; *Gurnis et al.*, 2004]. *Maffione et al.* [2015a] showed that oceanic detachment faults next to mid-ocean ridges are the ideal locus of subduction initiation upon ridge inversion. Oceanic detachments are cross-lithospheric fault zones that are ultraweak due to hydrothermal alteration (serpentinization) [e.g., *MacLeod et al.*, 2002; *Escartín et al.*, 2003; *Schroeder and John*, 2004; *Boschi et al.*, 2006], form at or close and parallel to slow or ultraslow spreading axes, dip toward them, and can tectonically accommodate most or all of plate divergence [e.g., *Reston et al.*, 2001; *MacLeod et al.*, 2002, 2009; *Smith et al.*, 2006; *Escartin et al.*, 2008; *Reston and Ranero*, 2011]. Because every ridge will spread slowly just prior to its demise and subsequent inversion, detachments are likely present adjacent to every ridge that is inverted [*Maffione et al.*, 2015a]. Subduction initiation along a detachment then preserves a young, weak, trench-parallel spreading ridge within tens of kilometers of the incipient trench. This preserved ridge may then be reactivated upon overriding plate extension. This model of subduction initiation and SSZ ophiolite formation may successfully explain the chemostratigraphy of Jurassic Mirdita ophiolite of Albania. The Mirdita ophiolite preserves an oceanic detachment [*Nicolas et al.*, 1999; *Maffione et al.*, 2013] in MORB crust between the obduction front and SSZ crust [*Dilek et al.*, 2008], used by *Maffione et al.* [2015a] as key example where their scenario applies.

Intraoceanic subduction within the Neotethys that produced the Cretaceous Neotethyan SSZ ophiolite belt of Arabia and Anatolia [*Dilek et al.*, 2007; *Dilek and Furnes*, 2011], likely formed along both transform faults and ridge systems. Plate reconstructions of the Neotethys show paleo-spreading along E-W trending ridges [*Müller et al.*, 2008; *Gaina et al.*, 2013] with N-S trending transform faults [*Lippard et al.*, 1986; *Navabpour*

et al., 2014]. The dominantly north to north-east dipping subduction zones that formed below these ophiolites likely formed parallel to these ridges [*Hacker*, 1994; *Navabpour et al*., 2014]. An originally Late Cretaceous ∼N-S trending, highly oblique subduction zone below a Central Anatolian segment [*Lefebvre et al*., 2013; *Advokaat et al*., 2014] may, on the other hand, suggest transform inversion. Since ridges are normally segmented by transform faults [*Müller et al*., 2008], the two mechanisms of subduction initiation and arc SSZ spreading center formation are likely to work in tandem when the convergence direction that forces subduction initiation is oblique to the paleo-spreading direction [*Maffione et al*., 2015a].

## 5. An Integrated Working Hypothesis

5.1. SSZ Spreading, Mantle Wedge Volume Decrease, Slab Flattening, and Metamorphic Sole Formation

The typical inverse pressure gradient of soles shows that they were decompressed and exhumed during their downward growth [*Jamieson*, 1986; *Gnos*, 1998]. Previous explanations inferred exhumation in a narrow channel along the subduction plate contact [*Wakabayashi and Dilek*, 2000] analogous to HP-LT subduction channels [*Jolivet et al*., 2003] or HT extrusion wedges like the Greater Himalaya [*Hodges et al*., 1992; *Grujic et al*., 1996]. Such settings, however, also display extensional detachment faults with normal PT gradients at the top that accommodated their upward motion relative to the overburden [*Hodges et al*., 1992; *Grujic et al*., 1996; *Jolivet et al*., 2003]. Metamorphic soles do generally not have such low-grade shear zones at their top. Moreover, soles are found below ophiolites as far as 100 km away from the obduction front, whereas wedges and channels would be found at the obduction front, cutting the ophiolite section [*Dewey and Casey*, 2011, 2013]. Soles are pierced by mafic dykes with ages similar to, and also much younger than sole exhumation [*Lytwyn and Casey*, 1995; *Hacker et al*., 1996; *Hacker and Gnos*, 1997; *Çelik*, 2008] showing that after their exhumation soles overlie mantle again, which is not expected at an obduction front. Finally, the similar pressures for the top of a sole as for the peridotites immediately overlying the sole [*Spray et al*., 1984; *Jamieson*, 1986], and the granulite-facies metasediments wedged within the mantle section of the UAE ophiolite [*Gnos and Kurz*, 1994; *Gnos and Peters*, 1995] suggest that a significant pressure gap, or gradient, lies between the base of the mantle section and the SSZ ophiolitic crust, and not between the sole and the mantle section. All of these features indicate that the mantle and oceanic crust above the sole thins during sole formation, i.e. that the plate contact (and thus the slab) flattens [*Dewey and Casey*, 2013].

The conclusions drawn from sole formation and exhumation are, in fact, straightforwardly compatible with the magmatic and kinematic history of SSZ ophiolite formation, as illustrated in the cartoons of Figure 3. Slab flattening to exhume the sole requires that the thickness of the overlying mantle wedge decreases. With constant volume of the mantle wedge, this would require an increase of the original area above the mantle wedge. This is consistent with SSZ spreading, which requires seafloor spreading above a nascent subduction zone at the expense of the underlying mantle wedge (Figures 3b and 3c)—through magmatic depletion of that wedge [*Pearce et al*., 1984] and, if that is not or no longer possible, by fault-controlled spreading [*Girardeau and Mercier*, 1988; *Maffione et al*., 2015b].

We, therefore, propose that metamorphic soles are formed and exhumed synchronously with, and as a direct consequence of spreading above a nascent subduction zone (Figure 3c). This spreading leads to mantle wedge ultradepletion by melt extraction (creating boninites), likely in combination with or followed by fault-assisted spreading, and consequent mantle wedge thinning. This explains why ultradepleted mantle sections of ophiolites are presently at much shallower depths than when melt was extracted from it. The consistency of the ages of the metamorphic sole, as well as the ophiolitic crust, along ophiolite belts of thousands of kilometers long, suggests that both sole exhumation and SSZ magmatism are short-lived episodes (few millions of years) as previously inferred [*Stern et al*., 2012]. After sole exhumation due to SSZ spreading, (i) the maturing slab decouples from the upper plate along the existing plate contact, which is located between the exhumed metamorphic sole and the downgoing plate, (ii) the slab steepens due to incipient slab pull, (iii) asthenospheric material flows in between the sole and the slab, and (iv) generates arc-magmatic dyke intrusion into the sole and the overlying lithospheric mantle (Figure 3d). Enhanced overriding plate extension associated with this event will, in the case of ridge-parallel subduction initiation be accommodated along the same ridge that produced the fore-arc ophiolites, but which migrated away from the trench into a back-arc position (Figure 3d). In the case of transform-parallel subduction initiation, this extension may generate a new back-arc spreading center.
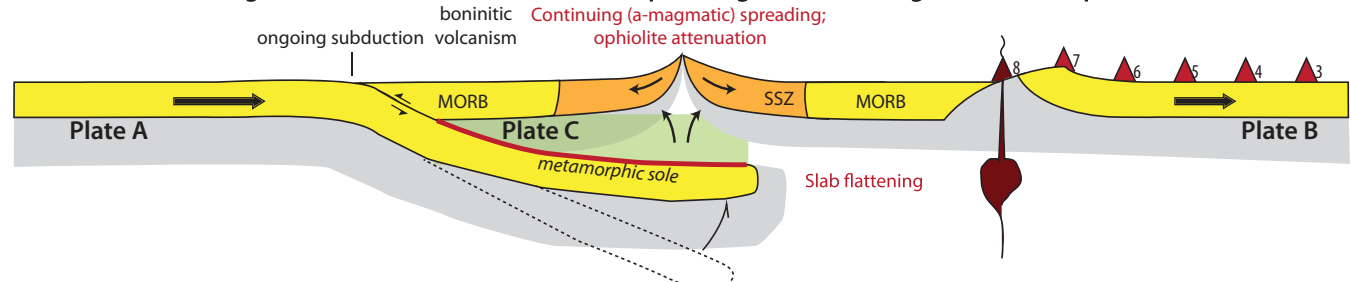
STAGE 1: Slowing of ocean spreading rates preceding ridge inversion
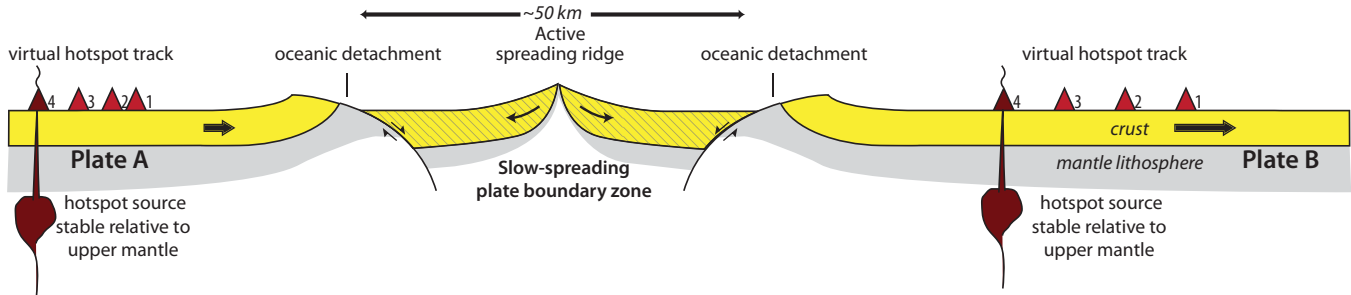
STAGE 2: Slow-spreading ridge (or transform) inversion; overriding plate spreading above nascent slab mantle anchor
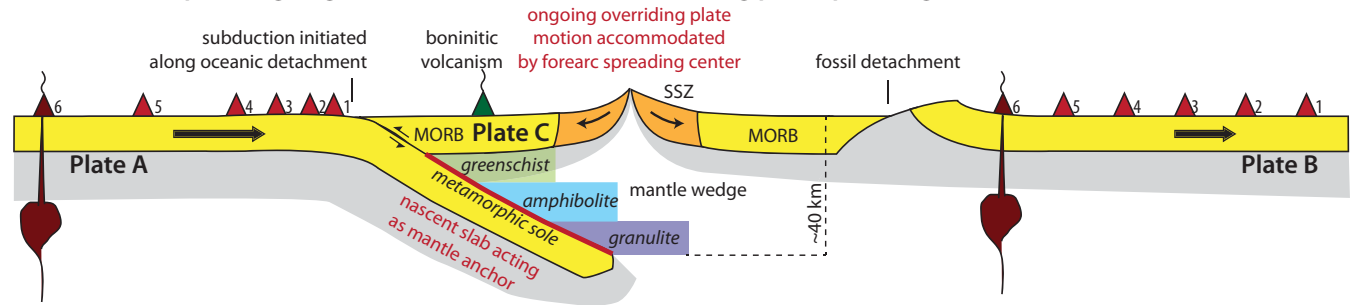
STAGE 3: Mantle wedge volume decrease due to forearc spreading: slab flattening and metamorphic sole exhumation

STAGE 4: Initiation slab pull: slab steepening, inflow of mantle below and dyke intrusion into sole; stable subduction
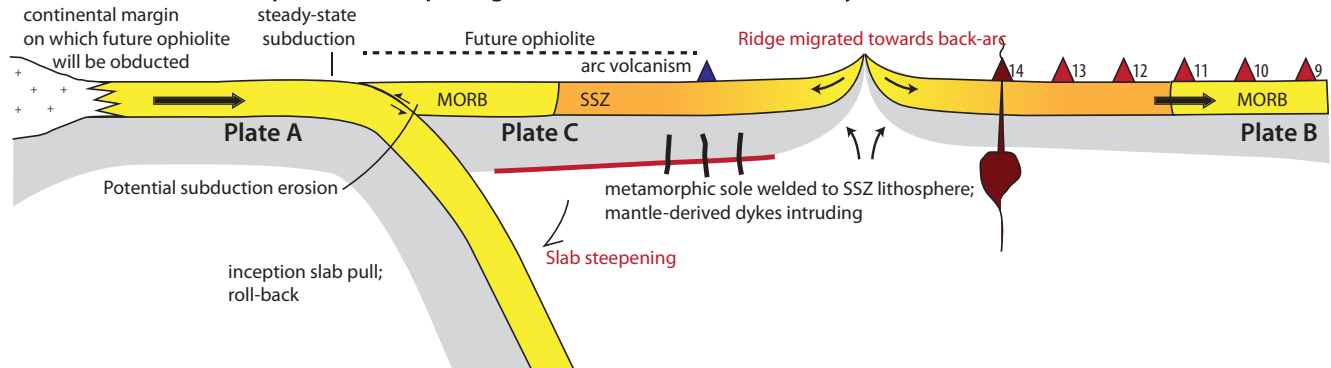

Figure 3. Typical cross-sectional evolution of intraoceanic subduction initiation and suprasubduction zone ophiolite formation, drawn N-S over the plate kinematic configuration illustrated. Motions shown in a hypothetical mantle reference frame illustrated with hot spot tracks on plates A and B. (a) Immediately before cessation of spreading and ridge inversion, slow spreading will lead to off-axis oceanic detachment formation. (b) Detachment inversion starts subduction upon forced convergence. Slab anchoring in the asthenosphere slows down or halts the motion of the trench relative to the mantle. Ongoing overriding plate motion then generates overriding plate extension, reactivation of the ridge preserved in the fore arc, and the formation of suprasubduction zone oceanic crust at the expense of the underlying mantle wedge. (c) This leads to ultradepletion, and likely tectonic exhumation of the mantle wedge associated with fore-arc area increase, thinning the mantle wedge, and shallowing of the slab. At the plate contact, rocks from the top of the nascent slab are welded to the base of the hot mantle section to form a metamorphic sole, which as a consequence of slab shallowing develops a typical inverted pressure-temperature gradient. (d) Upon eclogitization in the nascent slab creating negative buoyancy, slab pull starts and the slab decouples from the sole and steepens. This leads to asthenospheric inflow into the mantle wedge, reflected in the intrusion of mafic dykes into the sole and the overlying lithospheric mantle. Suprasubduction zone ophiolites are formed upon arrival of a buoyant collider, e.g., a passive margin, in the subduction zone, and the consequent uplift of the fore arc.

5.2. Absolute Plate Motions, Subduction Initiation, and Fore-Arc Extension

Metamorphic sole exhumation and SSZ ophiolite formation requires a phase of overriding plate extension intrinsically related to subduction initiation, during which time the nascent slab can flatten. If subduction initiates along a transform fault below an active ridge this spreading will produce SSZ oceanic crust, decreasing the volume of the mantle wedge below the spreading ridge, leading to slab flattening if the geodynamic mechanism that drove spreading to begin with continues to exist [*Karig*, 1982; *Dewey and Casey*, 2011]. Overriding plate extension following ridge, or off-ridge detachment inversion is inferred to result from slab rollback [*Hawkins et al.*, 1984; *Leitch*, 1984; *Edelman*, 1988; *Dilek and Furnes*, 2011]. Slab rollback is the process in which the slab subduction rate into the upper mantle exceeds the horizontal velocity of the subducting plate relative to the mantle, resulting in slab retreat relative to, and though the mantle. Rollback, however, usually steepens the slab, and may generate SSZ ophiolites without metamorphic soles, or with metamorphic sole fragments exclusively found in subduction channel mélanges [e.g., *Guilmette et al.*, 2012], but it cannot explain a sole's inverted pressure gradient.

Numerical models of forced subduction initiation in response to far-field stress changes associated with global plate reorganizations [*Agard et al.*, 2007], however, invoke a period of forced underthrusting of one plate below another [*Mueller and Phillips*, 1991; *Toth and Gurnis*, 1998; *Hall et al.*, 2003]. In these models, the negative buoyancy of the lithosphere is initially too small and density-enhancing, dehydrating metamorphic reactions are invoked, like eclogitization, in the underthrusted lithosphere to develop slab pull. Only once that happened, subduction rates increase and can accelerate plate convergence or lead to slab rollback and overriding plate extension. Numerical simulations [*Toth and Gurnis*, 1998; *Hall et al.*, 2003; *Leng and Gurnis*, 2011; *Chertova et al.*, 2014], laboratory studies [*Faccenna et al.*, 1999], and tectonic reconstructions [*van Hinsbergen et al.*, 2014] suggest that slab pull may start after ~100 km of forced underthrusting. These models included lithosphere that is much older than the very young lithosphere that would start subducting after ridge inversion. After oceanic detachment fault inversion, the nascent slab is even more buoyant than in the models above, and the amount of lithosphere that in this case needs to be subducted before the inception of slab pull may thus be different. Nevertheless, subduction initiation-related overriding plate extension and associated slab flattening likely occurs in the narrow time window, starting when the nascent slab reaches a depth that is at least equivalent to the typical peak pressures recorded in the top of the metamorphic sole (10–15 kbar, ~30–45 km, Figure 2) and ending with the onset of slab pull, slab steepening, and self-sustaining subduction.

To identify a potential mechanism that may generate overriding plate extension during forced convergence, we view the subduction initiation problem in a mantle reference frame (Figures 3 and 4). Generic numerical and analogue models of subduction initiation tend to keep the future overriding plate, and the weakness zone along which subduction initiates, stationary relative to the upper mantle [e.g., *Leng and Gurnis*, 2011]. Moving hot spot reference frames [e.g., *O'Neill et al.*, 2005; *Doubrovine et al.*, 2012], however, show that mid-ocean ridges and transform faults almost always move relative to the deeper mantle. For example, the mid-Cretaceous Neotethyan intraoceanic subduction zones that formed north of Africa and Arabia, ~100 Ma ago, must have been moving ~2–3 cm/yr northward with the African plate relative to the mantle at the moment of subduction initiation. Initiation of subduction was associated with an acceleration of the absolute African plate motion to ~4 cm/yr [*Doubrovine et al.*, 2012], coinciding with a global plate reorganization [*Agard et al.*, 2006; *Monié and Agard*, 2009; *Matthews et al.*, 2012]. If the plate north of the Neotethyan spreading ridge accelerated less, the former ridge becomes a convergent plate boundary, with the nascent subduction zone moving northward relative to the underlying upper mantle (Figures 3 and 4).

The example in Figures 3 and 4 illustrates how absolute plate motions can play a key role in explaining SSZ ophiolites. We explain this concept further in the cartoons of Figure 4. Our example contains two plates, A and B, separated by a slow spreading mid-oceanic ridge r, flanked by detachment faults d_a and d_b. Spreading centers and flanking oceanic detachments are generally symmetric [e.g., *Smith et al.*, 2006; *MacLeod et al.*, 2009]. If the ridge does not move relative to the upper mantle (UM) at the time of its inversion, as portrayed in the "stationary ridge" example in the right-hand panel of Figure 4a, both detachments have an equal chance to become a subduction zone and the newly formed overriding plate will be stationary relative to the mantle. If the ridge is undergoing absolute plate motion, however, i.e., if it is moving relative to the upper mantle as portrayed in the "moving ridge" example in the right-hand panel of Figure 4a, the newly formed overriding plate will move relative to the mantle. As a result, also the trench will initially
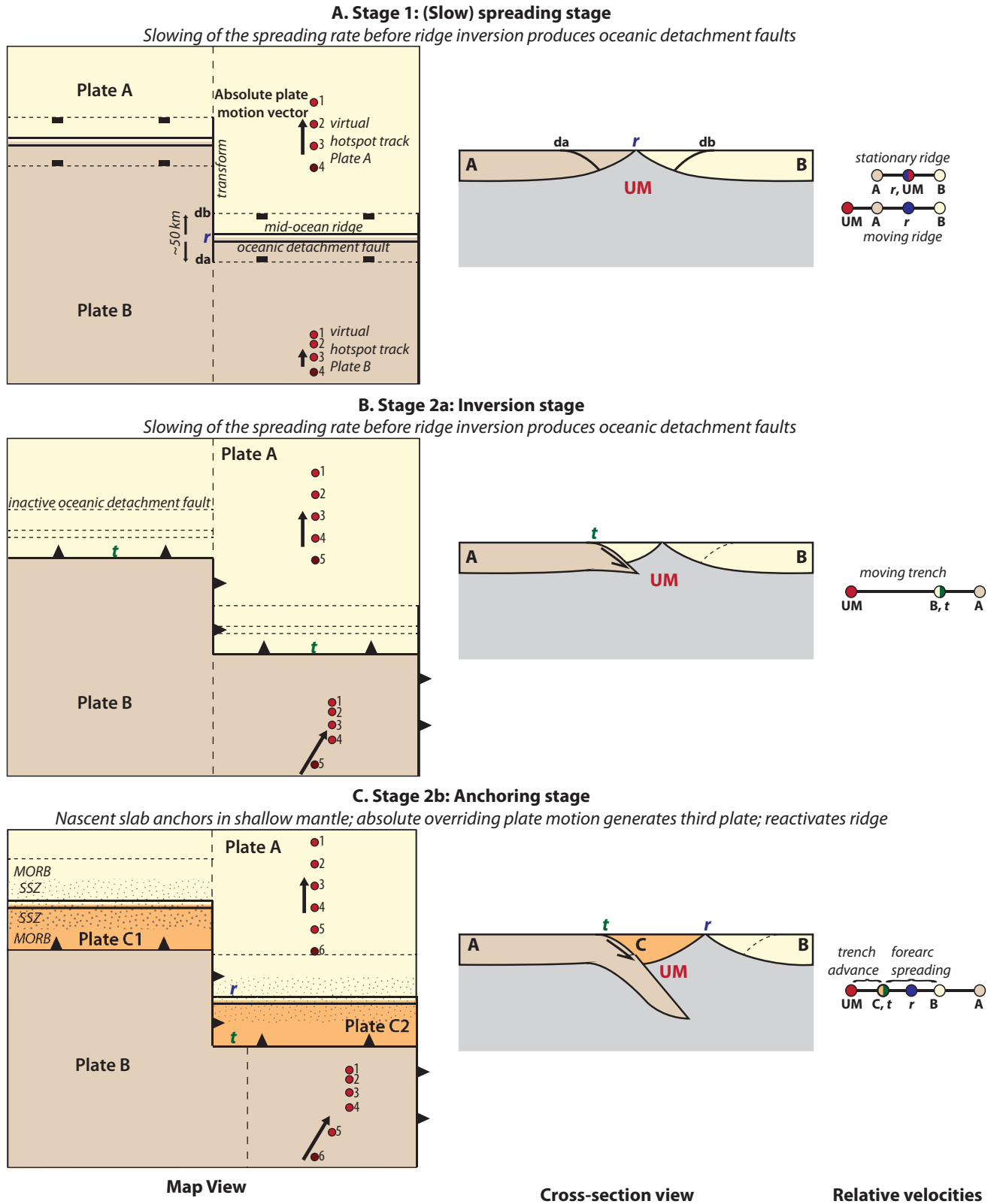
Figure 4. Schematic plate kinematic scenario of intraoceanic subduction initiation in a mantle reference frame. (left) Plates and plate boundaries, with absolute plate motions illustrated through virtual hot spot tracks, comparable to Figure 3. (middle) Plates in cross-sectional view. (right) Plates and plate boundaries on a velocity line [see e.g., *Cox and Hart*, 1986], in which a position of plate B to the right of plate A on the velocity line shows that plate B is moving to the right relative to plate A at a rate proportional to the distance between the points. Stage 1 represents the slow spreading stage that precedes intraoceanic subduction initiation. Stage 2a represents the inversion of off-ridge oceanic detachment faults and transforms upon forced, oblique convergence. Subduction will be favored in the direction of absolute plate motion (see Figure 3). Stage 2b: Inversion of a slow spreading ridge that moves relative to the mantle will generate an advancing trench *t* if plate B becomes the overriding plate. An advancing trench will experience resistance of the mantle that will lead to anchoring of the slab and stagnation of the trench. If the velocity of plate B does not change, or changes less, a third plate will form by reactivation of ridge *r*, which then forms a fore-arc spreading center that can generate a SSZ ophiolite.

move relative to the mantle at a rate that is equal to that of the overriding plate. In the example of Figure 4b, plate B becomes the overriding plate because of inversion of detachment d_a, and trench t moves with it. The nascent slab of plate A in this example dips in the direction of absolute plate motion and will experience resistance of the asthenosphere when it starts sinking. This may lead to a process we here define as "slab anchoring": the nascent slab will experience resistance against absolute plate motion from the asthenosphere, slowing down the motion of the trench t relative to the upper mantle UM (Figure 4c), and steepening the slab, even if it is less buoyant than the asthenosphere. One may compare this process with sticking a paddle in the water while moving with a canoe over a lake: that paddle will steepen even if it is more buoyant than water, resisting against the motion of the canoe. In velocity space, the trench t will no longer coincide with plate B, but instead move toward UM. If the absolute motion of overriding plate B does not change, or changes slower, trench stagnation or slowdown relative to the mantle requires the formation of a new, third plate C in the system, bounded by trench t from plate A at one end, and by reactivated spreading ridge r from plate B at the other.

In the Neotethyan example, the northern plate of the Neotethys subducted below Eurasia [*Agard et al.*, 2011; *Okay et al.*, 2013] and thus experienced slab pull that drove its ongoing northward motion. As a logical consequence, a weak, preserved mid-Neotethys ridge that would be preserved in the fore arc of the new, northward dipping intraoceanic subduction zone if subduction started by detachment inversion, reactivated when slab anchoring prohibited trench advance (Figure 4c). Conversely, absolute plate motion will work against development of a subducting slab that dips away from the absolute plate motion direction [*Rodríguez-González et al.*, 2014]. The Cretaceous intraoceanic subduction zones in the Neotethys all had a northward subduction polarity [*Stampfli and Borel*, 2002; *Agard et al.*, 2011; *Dilek and Furnes*, 2011], and thus support the notion that the subduction polarity tends to be toward the direction of absolute plate motion of the structure that is used for subduction initiation.

6. Outlook and Future Work

Ophiolite sequences provide the most direct access to rocks for the study of mid-ocean ridge structure and dynamics. Generally, even the thickest ophiolitic crust, however, is only 3 km thick [*Nicolas et al.*, 2000], less than half the thickness of crust underlying modern oceans as suggested by seismological constraints [*Moores*, 1982]. *Moores* [1982] already concluded that ophiolitic crust must have been strongly attenuated prior to or during obduction, which is paradoxical given the compressional nature of this process. If the scenario proposed here is valid, it may propose a (partial) solution for this paradox. Where ophiolitic crust is formed from a mantle wedge of only tens of kilometers deep, only a limited amount of melt can be generated despite the influx of subduction-related fluids. SSZ ophiolites may therefore not be entirely representative for seafloor spreading dynamics and the structure and composition of oceanic crust of "normal" mid-ocean ridges [e.g., *MacLeod et al.*, 2013]. For instance, nonmagmatic spreading centers accommodating spreading along detachments at mid-ocean ridges require (ultra) slow spreading to prevent the mantle from melting [*Escartin et al.*, 2008; *MacLeod et al.*, 2009]. In a suprasubduction zone setting, melting is likely limited by ultradepletion of the mantle wedge, regardless of the spreading rate. Fault-controlled spreading may well be the dominant mode of SSZ ophiolite extension [*Maffione et al.*, 2015b], and if melting of the mantle wedge was prohibited, the only mode of spreading is along extensional detachments, explaining why ∼90% of ophiolites expose only a "dismembered" Penrose sequence. We note that no ophiolite, even those with a complete Penrose sequence such as the Semail ophiolite of Oman is thicker than 10–12 km [*Nicolas et al.*, 2000], so even that ophiolite lost 70% or more of its original thickness indicated by the pressure recorded in the top of the metamorphic sole [*Hacker and Gnos*, 1997].

The geological record of ophiolites and their metamorphic soles has long been recognized as the key to understanding subduction initiation [*Moores*, 1982; *Casey and Dewey*, 1984; *Stern and Bloomer*, 1992]. Our scenario reinforces models advocating forced subduction initiation as a result of far-field force changes [*Toth and Gurnis*, 1998; *Hall et al.*, 2003; *Gurnis et al.*, 2004; *Agard et al.*, 2007, 2014; *Leng and Gurnis*, 2011]. A key question for future plate tectonic research is then which processes create those far-field forces driving subduction initiation. Previous work has called for global reorganizations [*Agard et al.*, 2007], but what causes these? Are they related to stress field changes associated with continent-

continent collisions, or with the arrival of mantle plumes below plates [*van Hinsbergen et al.*, 2011]? Do such stress changes need to occur on the plate adjacent to the new subduction zone, or can they propagate through the plate circuit? Explaining the processes that force subduction initiation may complete our understanding of the plate tectonic cycle and forms a key step toward a quantitative and dynamic explanation for plate tectonics.

References

Advokaat, E. L., D. van Hinsbergen, N. Kaymakcı, R. L. M. Vissers, and B. W. H. Hendriks (2014), Late Cretaceous extension and Palaeogene rotation-related contraction in Central Anatolia recorded in the Ayhan-Büyükkışla basin, *Int. Geol. Rev.*, *56*, 1813–1836.

Agard, P., P. Monié, W. Gerber, J. Omrani, M. Molinaro, B. Meyer, L. Labrousse, B. Vrielynck, L. Jolivet, and P. Yamato (2006), Transient, synob-duction exhumation of Zagros blueschists inferred from P-T, deformation, time, and kinematic constraints: Implications for Neotethyan wedge dynamics, *J. Geophys. Res.*, *111*, B11401, doi:10.1029/2005JB004103.

Agard, P., L. Jolivet, B. Vrielynck, E. Burov, and P. Monié (2007), Plate acceleration: The obduction trigger?, *Earth Planet. Sci. Lett.*, *258*(3–4), 428–441.

Agard, P., J. Omrani, L. Jolivet, H. Whitechurch, B. Vrielynck, W. Spakman, P. Monié, B. Meyer, and M. J. R. Wortel (2011), Zagros orogeny: A subduction-dominated process, *Geol. Mag.*, *148*, 692–725.

Agard, P., X. Zuo, F. Funiciello, N. Bellahsen, C. Faccenna, and D. Savva (2014), Obduction: Why, how and where. Clues from analog models, *Earth Planet. Sci. Lett.*, *393*, 132–145.

Atkinson, S. J. (1976), Ophiolite emplacement on to continental margins, *Nature*, *264*, 164–165.

Boschi, C., G. L. Früh-Green, A. Delacour, J. A. Karson, and D. S. Kelley (2006), Mass transfer and fluid flow during detachment faulting and development of an oceanic core complex, Atlantis Massif (MAR 30°N), *Geochem. Geophys. Geosyst.*, *7*, Q01004, doi:10.1029/2005GC001074.

Boudier, F., and R. G. Coleman (1981), Cross section through the peridotite in the Samail Ophiolite, southeastern Oman Mountains, *J. Geophys. Res.*, *86*, 2573–2592.

Boudier, F., G. Ceulener, and A. Nicolas (1988), Shear zones, thrusts and related magmatism in the Oman ophiolite: Initiation of thrusting on an oceanic ridge, *Tectonophysics*, *151*, 275–296.

Casey, J. F., and J. F. Dewey (1984), Initiation of subduction zones along transform and accreting plate boundaries, triple-junction evolution, and forearc spreading centres—Implications for ophiolitic geology and obduction, *Geol. Soc. Spec. Publ.*, *13*(1), 269–290.

Çelik, Ö. F. (2007), Metamorphic sole rocks and their mafic dykes in the eastern Tauride belt ophiolites (southern Turkey): Implications for OIB-type magma generation following slab break-off, *Geol. Mag.*, *144*, 849–866.

Çelik, Ö. F. (2008), Detailed geochemistry and K-Ar geochronology of the metamorphic sole rocks and their mafic dykes from the Mersin Ophiolite, Southern Turkey, *Turk. J. Earth Sci.*, *17*, 685–708.

Çelik, Ö. F., M. F. Delaloye, and G. Feraud (2006), Precise ^{40}Ar-^{39}Ar ages from the metamorphic sole rocks of the Tauride Belt Ophiolites, southern Turkey: Implications for the rapid cooling history, *Geol. Mag.*, *143*, 213–227.

Chertova, M. V., W. Spakman, A. P. van den Berg, T. Geenen, and D. J. J. van Hinsbergen (2014), Underpinning tectonic reconstructions of the western Mediterranean region through dynamic slab evolution from 3D numerical modeling, *J. Geophys. Res.*, *119*, 5876–5902, doi:10.1002/2014JB011150.

Coleman, R. G. (1971), Plate tectonic emplacement of upper mantle peridotites along continental edges, *J. Geophys. Res.*, *76*, 1212–1222.

Cox, A., and R. B. Hart (1986), *Plate Tectonics, How It Works*, John Wiley, U. K.

Dewey, J. F. (1976), Ophiolite obduction, *Tectonophysics*, *31*, 93–120.

Dewey, J. F., and J. M. Bird (1971), Origin and emplacement of the ophiolite suite: Appalachian ophiolites in Newfoundland, *J. Geophys. Res.*, *76*, 3179–3206.

Dewey, J. F., and J. F. Casey (2011), The origin of obducted large-slab ophiolite complexes, in *Arc-Continent Collision. Frontiers in Earth Sciences*, edited by D. Brown and P. D. Ryan, pp. 431–444, Springer-Verlag, Berlin Heidelberg.

Dewey, J. F., and J. F. Casey (2013), The sole of an ophiolite: The Ordovician Bay of Islands Complex, Newfoundland, *J. Geol. Soc.*, *170*, 715–722.

Dewey, J. F., W. C. Pitman, W. B. F. Ryan, and J. Bonnin (1973), Plate tectonics and the evolution of the alpine system, *Geol. Soc. Am. Bull.*, *84*, 3137–3180.

Dick, H. J., and T. Bullen (1984), Chromian spinel as a petrogenetic indicator in abyssal and alpine-type peridotites and spatially associated lavas, *Contrib. Mineral. Petrol.*, *86*, 54–76.

Dilek, Y., and H. Furnes (2011), Ophiolite genesis and global tectonics: Geochemical and tectonic fingerprinting of ancient oceanic lithosphere, *Geol. Soc. Am. Bull.*, *123*(3–4), 387–411.

Dilek, Y., and D. L. Whitney (1997), Counterclockwise P-T-t trajectory from the metamorphic sole of a Neo-Tethyan ophiolite (Turkey), *Tectonophysics*, *280*, 295–310.

Dilek, Y., H. Furnes, and M. Shallo (2007), Suprasubduction zone ophiolite formation along the periphery of Mesozoic Gondwana, *Gondwana Res.*, *11*, 453–475.

Dilek, Y., H. Furnes, and M. Shallo (2008), Geochemistry of the Jurassic Mirdita Ophiolite (Albania) and the MORB to SSZ evolution of a marginal basin oceanic crust, *Lithos*, *100*, 174–209.

Dimo-Lahitte, A., P. Monié, and P. Vergély (2001), Metamorphic soles from the Albanian ophiolites: Petrology, ^{40}Ar/^{39}Ar geochronology, and geodynamic evolution, *Tectonics*, *20*, 78–96.

Doubrovine, P. V., B. Steinberger, and T. H. Torsvik (2012), Absolute plate motions in a reference frame defined by moving hot spots in the Pacific, Atlantic, and Indian oceans, *J. Geophys. Res.*, *117*, B09101, doi:10.1029/2011JB009072.

Edelman, S. H. (1988), Ophiolite generation and emplacement by rapid subduction hinge retreat on a continent-bearing plate, *Geology*, *16*, 311–313.

Elitok, Ö., and K. Drüppel (2008), Geochemistry and tectonic significance of metamorphic sole rocks beneath the Beyşehir-Hoyran ophiolite (SW-Turkey), *Lithos*, *100*, 322–353.

Escartín, J., C. Mével, C. J. MacLeod, and A. M. McCaig (2003), Constraints on deformation conditions and the origin of oceanic detach-ments: The Mid-Atlantic Ridge core complex at 15–45°N, *Geochem. Geophys. Geosyst.*, *4*(8), 1067, doi:10.1029/2002GC000472.

Escartin, J., D. K. Smith, J. Cann, H. Schouten, C. H. Langmuir, and S. Escrig (2008), Central role of detachment faults in accretion of slow-spreading oceanic lithosphere, *Nature*, *455*, 790–794.

Faccenna, C., D. Giardini, P. Davy, and A. Argentieri (1999), Initiation of subduction at Atlantic-type margins: Insights from laboratory experiments, *J. Geophys. Res.*, *104*, 2749–2766.

Gaina, C., T. H. Torsvik, D. J. J. van Hinsbergen, S. Medvedev, S. C. Werner, and C. Labails (2013), The African Plate: A history of oceanic crust accretion and subduction since the Jurassic, *Tectonophysics*, *604*, 4–25.

Gaina, C., D. J. J. van Hinsbergen, and W. Spakman (2015), Tectonic interactions between India and Arabia since the Jurassic reconstructed from marine geophysics, ophiolite geology, and seismic tomography, *Tectonics*, 34, doi:10.1002/2014TC003780.

Geotimes (1972), Penrose field conference on ophiolites, *Geotimes*, *17*, 24–25.

Girardeau, J., and J.-C. Mercier (1988), Petrology and texture of the ultramafic rocks of the Xigaze ophiolite (Tibet): Constraints for mantle structure beneath slow-spreading ridges, *Tectonophysics*, *147*, 33–58.

Gnos, E. (1998), Peak metamorphic conditions of garnet amphibolites beneath the Semail ophiolite: Implications for an inverted pressure gradient, *Int. Geol. Rev.*, *40*, 281–304.

Gnos, E., and D. Kurz (1994), Sapphirine-quartz and sapphirine-corundum assemblages in metamorphic rocks associated with the Semail ophiolite (United Arab Emirates), *Contrib. Mineral. Petrol.*, *116*, 398–410.

Gnos, E., and T. Peters (1995), Tephroite-hausmannite-galaxite from a granulite-facies manganese rock of the United Arab Emirates, *Contrib. Mineral. Petrol.*, *120*, 372–377.

Gnos, E., A. Immenhauser, and T. Peters (1997), Late Cretaceous/early Tertiary convergence between the Indian and Arabian plates recorded in ophiolites and related sediments, *Tectonophysics*, *271*, 1–19.

Grujic, D., M. Casey, C. Davidson, L. C. Hollister, R. Kündig, T. L. Pavlis, and S. M. Schmid (1996), Ductile extrusion of the higher Himalayan crystalline in Bhutan: Evidence from quartz microfabrics, *Tectonophysics*, *260*, 21–43.

Guilmette, C., R. Hébert, C. Dupuis, C. Wang, and Z. Li (2008), Metamorphic history and geodynamic significance of high-grade metabasites from the ophiolitic mélange beneath the Yarlung Zangbo ophiolites, Xigaze area, Tibet, *J. Asian Earth Sci.*, *2008*, 423–437.

Guilmette, C., R. Hébert, C. Wang, and M. Villeneuve (2009), Geochemistry and geochronology of the metamorphic sole underlying the Xigaze Ophiolite, Yarlung Zangbo Suture Zone, South Tibet, *Lithos*, *112*, 149–162.

Guilmette, C., R. Hébert, J. Dostal, A. Indares, T. Ullrich, É. Bédard, and C. Wang (2012), Discovery of a dismembered metamorphic sole in the Saga ophiolitic mélange, South Tibet: Assessing an Early Cretaceous disruption of the Neo-Tethyan supra-subduction zone and consequences on basin closing, *Gondwana Res.*, *22*, 398–414.

Gurnis, M., C. Hall, and L. Lavier (2004), Evolving force balance during incipient subduction, *Geochem. Geophys. Geosyst.*, *5*, Q07001, doi:10.1029/2003GC000681.

Hacker, B. R. (1990), Simulation of the metamorphic and deformational history of the metamorphic sole of the Oman ophiolite, *J. Geophys. Res.*, *95*, 4895–4907.

Hacker, B. R. (1991), The role of deformation in the formation of metamorphic gradients: Ridge subduction beneath the Oman ophiolite, *Tectonics*, *10*, 455–473.

Hacker, B. R. (1994), Rapid emplacement of young oceanic lithosphere: Argon geochronology of the Oman ophiolite, *Science*, *265*, 1563–1565.

Hacker, B. R., and E. Gnos (1997), The conundrum of Samail: Explaining the metamorphic history, *Tectonophysics*, *279*, 215–226.

Hacker, B. R., J. L. Mosenfelder, and E. Gnos (1996), Rapid emplacement of the Oman ophiolite: Thermal and geochronologic constraints, *Tectonics*, *15*, 1230–1247.

Hall, C. E., M. Gurnis, M. Sdrolias, L. L. Lavier, and R. D. Müller (2003), Catastrophic initiation of subduction following forced convergence across fracture zones, *Earth Planet. Sci. Lett.*, *212*, 15–30.

Hawkins, J. W., S. H. Bloomer, C. A. Evans, and J. T. Melchior (1984), Evolution of intra-oceanic arc-trench systems, *Tectonophysics*, *102*, 175–205.

Hébert, R., R. Bezard, C. Guilmette, J. Dostal, C. Wang, and Z. F. Liu (2012), The Indus-Yarlung Zangbo ophiolites from Nanga Parbat to Namche Barwa syntaxes, southern Tibet: First synthesis of petrology, geochemistry, and geochronology with incidences on geodynamic reconstructions of Neo-Tethys, *Gondwana Res.*, *22*, 377–397.

Hess, H. H. (1965), Mid-oceanic ridges and tectonics of the sea-floor, *Submar. Geol. Geophys.*, *17*, 317–334.

Hickey, R. L., and F. A. Frey (1982), Geochemical characteristics of boninite series volcanics: Implications for their source, *Geochim. Cosmochim. Acta*, *46*, 2099–2115.

Hirose, K., and T. Kawamoto (1995), Hydrous partial melting of lherzolite at 1 GPa: The effect of H_2O on the genesis of basaltic magmas, *Earth Planet. Sci. Lett.*, *133*, 463–473.

Hodges, K. V., R. R. Parrish, T. B. Housh, D. R. Lux, B. C. Burchfiel, L. H. Royden, and Z. Chen (1992), Simultaneous Miocene extension and shortening in the Himalayan orogen, *Science*, *258*, 1466–1470.

Ishikawa, T., K. Nagaishi, and S. Umino (2002), Boninitic volcanism in the Oman ophiolite: Implications for thermal condition during transition from spreading ridge to arc, *Geology*, *30*, 899–902.

Jamieson, R. A. (1980), Formation of metamorphic aureoles beneath ophiolites—Evidence from the St. Anthony Complex, Newfoundland, *Geology*, *8*(3), 150–154.

Jamieson, R. A. (1986), P-T paths from high-temperature shear zones beneath ophiolites, *J. Metamorph. Geol.*, *4*, 3–22.

Johnson, M. C., and T. Plank (1999), Dehydration and melting experiments constrain the fate of subducted sediments, *Geochem. Geophys. Geosyst.*, *1*(12), 1007, doi:10.1029/1999GC000014.

Jolivet, L., C. Facenna, B. Goffé, E. Burov, and P. Agard (2003), Subduction tectonics and exhumation of high-pressure metamorphic rocks in the Mediterranean orogen, *Am. J. Sci.*, *303*, 353–409.

Kakar, M. I., M. Khan, and K. Mahmood (2014), Facies and distribution of metamorphic rocks beneath the Muslim Bagh ophiolite (NW Pakistan): Tectonic implications, *J. Himalayan Earth Sci.*, *47*, 115–124.

Kapsiotis, A. N. (2014), Compositional signatures of SSZ-type peridotites from the northern Vourinos ultra-depleted upper mantle suite, NW Greece, *Chem. Erde Geochem.*, *74*, 783–801.

Karig, D. E. (1982), Initiation of subduction zones: Implications for arc evolution and ophiolite development, *Geol. Soc. Spec. Publ.*, *10*, 563–576.

Kostopoulos, D. K., and B. J. Murton (1992), Origin and distribution of components in boninite genesis: Significance of the OIB component, *Geol. Soc. Spec. Publ.*, *60*, 133–154.

Lefebvre, C., M. J. M. Meijers, N. Kaymakci, A. Peynircioğlu, C. G. Langereis, and D. J. J. van Hinsbergen (2013), Reconstructing the geometry of central Anatolia during the late Cretaceous: Large-scale Cenozoic rotations and deformation between the Pontides and Taurides, *Earth Planet. Sci. Lett.*, *366*, 83–98.

Leitch, E. C. (1984), Island arc elements and arc-related ophiolites, *Tectonophysics*, *106*, 177–203.

Leng, W., and M. Gurnis (2011), Dynamics of subduction initiation with different evolutionary pathways, *Geochem. Geophys. Geosyst.*, *12*, Q12018, doi:10.1029/2011GC003877.

Lippard, S. J., A. W. Shelton, and I. G. Gass (1986), The ophiolite of northern Oman, *Geol. Soc. Mem.*, *11*, 170.

Lytwyn, J. N., and J. F. Casey (1995), The geochemistry of postkinematic mafic dike swarms and subophiolitic metabasites, Pozanti-Karsanti ophiolite, Turkey: Evidence for ridge subduction, *Geol. Soc. Am. Bull.*, *107*, 830–850.

MacLeod, C. J., S. Allerton, I. G. Gass, and C. Xenophontos (1990), Structure of a fossil ridge-transform intersection in the Troodos ophiolite, *Nature*, *348*, 717–720.

MacLeod, C. J., et al. (2002), Direct geological evidence for oceanic detachment faulting: The Mid-Atlantic Ridge, 15°45′N, *Geology*, *30*, 879–882.

MacLeod, C. J., R. C. Searle, B. J. Murton, J. F. Casey, C. Mallows, S. C. Unsworth, K. L. Achenbach, and M. Harris (2009), Life cycle of oceanic core complexes, *Earth Planet. Sci. Lett.*, *287*, 333–344.

MacLeod, C. J., J. C. Lissenberg, and L. E. Bibby (2013), "Moist MORB" axial magmatism in the Oman ophiolite: The evidence against a mid-ocean ridge origin, *Geology*, *41*(4), 459–462, doi:10.1130/G33904.1.

Maffione, M., A. Morris, and M. W. Anderson (2013), Recognizing detachment-mode seafloor spreading in the deep geological past, *Sci. Rep.*, *3*, 2336, doi:10.1038/srep02336.

Maffione, M., C. Thieulot, D. J. J. van Hinsbergen, A. Morris, O. Plumper, and W. Spakman (2015a), Dynamics of intra-oceanic subduction initiation. 1: Oceanic detachment fault inversion and the formation of forearc ophiolites, *Geochem. Geophys. Geosyst.*, doi:10.1002/2015GC005746.

Maffione, M., D. J. J. van Hinsbergen, L. Koornneef, C. Guilmette, K. V. Hodges, N. Borneman, W. Huang, L. Ding, and P. Kapp (2015b), Fore-arc hyperextension dismembered the South Tibetan ophiolites, *Geology*, doi:10.1130/G36472.1, in press.

Mahmood, K., F. Boudier, E. Gnos, P. Monié, and A. Nicolas (1995), ^{40}Ar/^{39}Ar dating of the emplacement of the Muslim Bagh ophiolite, Pakistan, *Tectonophysics*, *250*, 169–181.

Malpas, J. (1979), Dynamothermal aureole of the Bay of Islands ophiolite suite, *Can. J. Earth Sci.*, *16*, 2086–2101.

Matthews, K. J., M. Seton, and R. D. Müller (2012), A global-scale plate reorganization event at 105–100 Ma, *Earth Planet. Sci. Lett.*, *355–356*, 283–298.

McKenzie, D. P., and R. L. Parker (1967), The North Pacific: An example of tectonics on a sphere, *Nature*, *216*, 1276–1280.

McQuarrie, N., and D. J. J. van Hinsbergen (2013), Retrodeforming the Arabia-Eurasia collision zone: Age of collision versus magnitude of continental subduction, *Geology*, *41*, 315–318.

Miyashiro, A. (1973), The Troodos ophiolitic complex was probably formed in an island arc, *Earth Planet. Sci. Lett.*, *19*, 218–224.

Monié, P., and P. Agard (2009), Coeval blueschist exhumation along thousands of kilometers: Implications for subduction channel processes, *Geochem. Geophys. Geosyst.*, *10*, Q07002, doi:10.1029/2009GC002428.

Moores, E. M. (1982), Origin and emplacement of ophiolites, *Rev. Geophys.*, *20*, 735–760.

Moores, E. M., P. T. Robinson, J. Malpas, and C. Xenophonotos (1984), Model for the origin of the Troodos massif, Cyprus, and other mideast ophiolites, *Geology*, *12*, 500–503.

Mueller, S., and R. J. Phillips (1991), On the initiation of subduction, *J. Geophys. Res.*, *96*, 651–665.

Müller, R. D., M. Sdrolias, C. Gaina, and W. R. Roest (2008), Age, spreading rates, and spreading asymmetry of the world's ocean crust, *Geochem. Geophys. Geosyst.*, *9*, Q04006, doi:10.1029/2007GC001743.

Myhill, R. (2011), Constraints on the evolution of the Mesohellenic Ophiolite from subophiolitic metamorphic rocks, *Geol. Soc. Am. Spec. Pap.*, *480*, 75–94.

Navabpour, P., E. Barrier, and H. McQuillan (2014), Oblique oceanic opening and passive margin irregularity, as inherited in the Zagros fold-and-thrust belt, *Terra Nova*, *26*(3), 208–215.

Nicolas, A. (1989), *Structures of Ophiolites and Dynamics of Oceanic Lithosphere*, 360 pp., Kluwer Acad., Dordrecht, Netherlands.

Nicolas, A., F. Boudier, and A. Meshi (1999), Slow spreading accretion and mantle denudation in the Mirdita ophiolite (Albania), *J. Geophys. Res.*, *104*, 15,155–15,167.

Nicolas, A., F. Boudier, B. Ildefonse, and E. Ball (2000), Accretion of Oman and United Arab Emirates ophiolite—Discussion of a new structural map, *Mar. Geophys. Res.*, *21*, 147–179.

Okay, A. I., G. Sunal, S. Sherlock, D. Altıner, O. Tüysüz, A. R. C. Kylander-Clark, and M. Aygül (2013), Early Cretaceous sedimentation and orogeny on the active margin of Eurasia: Southern Central Pontides, Turkey, *Tectonics*, *32*, 1247–1271, doi:10.1002/tect.20077.

O'Neill, C., D. Müller, and B. Steinberger (2005), On the uncertainties in hot spot reconstructions and the significance of moving hot spot reference frames, *Geochem. Geophys. Geosyst.*, *6*, Q04003, doi:10.1029/2004GC000784.

Pagé, P., J. H. Bedard, and A. Tremblay (2009), Geochemical variations in a depleted fore-arc mantle: The Ordovician Thetford Mines Ophiolite, *Lithos*, *113*, 21–47.

Pearce, J. A. (2003), Supra-subduction zone ophiolites: The search for modern analogues, *Geol. Soc. Am. Spec. Pap.*, *373*, 269–293.

Pearce, J. A., S. J. Lippard, and S. Roberts (1984), Characteristics and tectonic significance of supra-subduction zone ophiolites, *Geol. Soc. Spec. Publ.*, *16*, 77–94.

Pearce, J. A., et al. (1992), Boninite and harzburgite from Leg 125 (Bonin-Mariana Forearc): A case study of magma genesis during the initial stages of subduction, in *Proceedings of Scientific Results, ODP, Leg 125, Bonin/Mariana Region*, pp. 623–662, U.S. Gov. Print. Off., Washington, D. C.

Plunder, A., P. Agard, C. Chopin, and A. I. Okay (2013), Geodynamics of the Tavşanlı zone, western Turkey: Insights into subduction/obduction processes, *Tectonophysics*, *608*, 884–903.

Rassios, A. H., and E. M. Moores (2006), Heterogeneous mantle complex, crustal processes, and obduction kinematics in a unified Pindos-Vourinos ophiolitic slab (northern Greece), *Geol. Soc. Spec. Publ.*, *260*, 237–266.

Reston, T. J., and C. R. Ranero (2011), The 3-D geometry of detachment faulting at mid-ocean ridges, *Geochem. Geophys. Geosyst.*, *12*, Q0AG05, doi:10.1029/2011GC003666.

Reston, T. J., J. Pennell, A. Stubenrauch, I. Walker, and M. Pérez-Gussinyé (2001), Detachment faulting, mantle serpentinization, and serpentinite-mud volcanism beneath the Porcupine Basin, southwest of Ireland, *Geology*, *29*, 587–590.

Rioux, M., B. Hacker, J. Mattinson, P. Kelemen, J. Blusztajn, and G. Gehrels (2007), Magmatic development of an intra-oceanic arc: High-precision U-Pb zircon and whole-rock isotopic analyses from the accreted Talkeetna arc, south-central Alaska, *Bull. Geol. Soc. Am.*, *119*, 1168–1184.

Rioux, M., S. Bowring, P. Kelemen, S. Gordon, F. Dudás, and R. Miller (2012), Rapid crustal accretion and magma assimilation in the Oman-U.A.E. ophiolite: High precision U-Pb zircon geochronology of the gabbroic crust, *J. Geophys. Res.*, *117*, B07201, doi:10.1029/2012JB009273.

Rioux, M., S. Bowring, P. Kelemen, S. Gordon, R. Miller, and F. Dudás (2013), Tectonic development of the Samail ophiolite: High-precision U-Pb zircon geochronology and Sm-Nd isotopic constraints on crustal growth and emplacement, *J. Geophys. Res.*, *118*, 2085–2101, doi: 10.1002/jgrb.50139.

Rodríguez-González, J., A. M. Negredo, and E. Carminati (2014), Slab-mantle flow interaction: Influence on subduction dynamics and duration, *Terra Nova*, *26*, 265–272.

Schroeder, T., and B. E. John (2004), Strain localization on an oceanic detachment fault system, Atlantis Massif, 30°N, Mid-Atlantic Ridge, *Geochem. Geophys. Geosyst.*, *5*, Q11007, doi:10.1029/2004GC000728.

Searle, M. P., and J. Cox (2002), Subduction zone metamorphism during formation and emplacement of the Semail ophiolite in the Oman Mountains, *Geol. Mag.*, *139*, 241–255.

Searle, M. P., and J. Malpas (1980), Structure and metamorphism of rocks beneath the Semail ophiolite of Oman and their significance in ophiolite obduction, *Trans. R. Soc. Edinburgh Earth Sci.*, *71*, 247–262.

Shervais, J. W. (1982), Ti-V plots and the petrogenesis of modern and ophiolitic lavas, *Earth Planet. Sci. Lett.*, *59*, 101–118.

Shervais, J. W. (2001), Birth, death, and resurrection: The life cycle of suprasubduction zone ophiolites, *Geochem. Geophys. Geosyst.*, *2*(1), 1010, doi:10.1029/2000GC000080.

Simonian, K. O., and I. G. Gass (1978), Arakapas fault belt, Cyprus: A fossil transform fault, *Geol. Soc. Am. Bull.*, *89*, 1220–1230.

Smith, D. K., J. R. Cann, and J. Escartín (2006), Widespread active detachment faulting and core complex formation near 13° N on the Mid-Atlantic Ridge, *Nature*, *442*, 440–443.

Šoštarić, S. B., A. L. Palinkaš, F. Neubauer, V. Cvetkovic, M. Bernroider, and J. Genser (2014), The origin and age of the metamorphic sole from the Rogozna Mts., Western Vardar Belt: New evidence for the one-ocean model for the Balkan ophiolites, *Lithos*, *192–195*, 39–55.

Spray, J. G., J. Bébien, D. C. Rex, and J. C. Roddick (1984), Age constraints on the igneous and metamorphic evolution of the Hellenic-Dinaric ophiolites, *Geol. Soc. Spec. Publ.*, *17*, 619–627.

Stampfli, G. M., and G. D. Borel (2002), A plate tectonic model for the Paleozoic and Mesozoic constrained by dynamic plate boundaries and restored synthetic oceanic isochrons, *Earth Planet. Sci. Lett.*, *196*, 17–33.

Stern, R. J. (2004), Subduction initiation: Spontaneous and induced, *Earth Planet. Sci. Lett.*, *226*, 275–292.

Stern, R. J., and S. H. Bloomer (1992), Subduction zone infancy: Examples from the Eocene Izu-Bonin-Mariana and Jurassic California arcs, *Geol. Soc. Am. Bull.*, *104*, 1621–1636.

Stern, R. J., M. Reagan, O. Ishizuka, Y. Ohara, and S. A. Whattam (2012), To understand subduction initiation, study forearc crust: To understand forearc crust, study ophiolites, *Lithosphere*, *4*, 469–483.

Stoneley, R. (1975), On the origin of ophiolite complexes in the southern Tethys region, *Tectonophysics*, *25*, 303–322.

Tilton, G. R., C. A. Hopson, and J. E. Wright (1981), Uranium-lead isotopic ages of the Samail Ophiolite, Oman, with applications to Tethyan ocean ridge tectonics, *J. Geophys. Res.*, *86*, 2763–2775.

Toth, J., and M. Gurnis (1998), Dynamics of subduction initiation at pre-existing fault zones, *J. Geophys. Res.*, *103*, 18,053–18,067.

van Hinsbergen, D. J. J., G. Steinberger, P. V. Doubrovine, and R. Gassmöller (2011), Acceleration and deceleration of India-Asia convergence since the Cretaceous: Roles of mantle plumes and continental collision, *J. Geophys. Res.*, *116*, B06101, doi:10.1020/2010JB008051.

van Hinsbergen, D. J. J., R. L. M. Vissers, and W. Spakman (2014), Origin and consequences of western Mediterranean subduction, rollback, and slab segmentation, *Tectonics*, *33*, 393–419, doi:10.1002/2013TC003349.

Wakabayashi, J., and Y. Dilek (2000), Spatial and temporal relationships between ophiolites and their metamorphic soles: A test of models of forearc ophiolite genesis, *Geol. Soc. Am. Spec. Pap.*, *349*, 53–64.

Wakabayashi, J., A. Ghatak, and A. R. Basu (2010), Suprasubduction-zone ophiolite generation, emplacement, and initiation of subduction: A perspective from geochemistry, metamorphism, geochronology, and regional geology, *Geol. Soc. Am. Bull.*, *122*, 1548–1568.

Warren, C. J., R. R. Parrish, D. J. Waters, and M. P. Searle (2005), Dating the geologic history of Oman's Semail ophiolite: Insights from U-Pb geochronology, *Contrib. Mineral. Petrol.*, *150*, 403–422.